NE 533 - MOOSE Project Report

Cecilia J. Harrison

Due Date: 25 April 2025

Name: Cecilia J. Harrison

Instructor: Dr. Benjamin W. Beeler

Contents

1. Introduction

1.1. Project Description

Idaho National Laboratory's Multiphysics Object Oriented Simulation Environment (MOOSE) has the capacity to utilize Finite Element Method (FEM) to examine properties of heat transfer, solid mechanics, and thermal expansion to provide information on fuel performance. [1]

In Part I of this project, four different MOOSE input scripts were utilized to analyze a one-dimensional problem of the heat transfer through a fuel pellet cross section from the centerline to the outer cladding. Both a steady-state and transient volumetric heating rate (VHR) as well as constant thermal conductivity coefficients and temperature-dependent coefficients were examined. The results are in reasonable agreement with the generally expected centerline temperatures for commercial nuclear reactors. [4]

1.2. Part I Deliverables

1. Outer cladding temperature is constant: 550 K
2. Solve temperature profile for:
3. Steady-state: LHR = 350 W/cm
4. Compare against analytical solution
5. Solve for centerline temperature vs time
6. Transient: LHR = $350*\exp(-((t-20)^2)/2)+350$
7. for up to t=100
8. Get peak T value
9. Use both a constant k and a temperature dependent k

In Part II of this project, one MOOSE input script was utilized to analyze a two-dimensional problem of the heat transfer through a fuel rod cross-section from the centerline to the outer cladding as well as accounting for the axial effects of the heating of the primary coolant and a non-homogeneous boundary condition of the outer cladding. A steady-state, axially dependent volumetric heating rate (VHR) as well as temperature-dependent thermal conductivity coefficients were applied. The results are in reasonable agreement with expected temperatures and radial and axial temperature profiles. [4]

1.3. Part II Deliverables

1. Fuel pin dimensions listed – 2D RZ
2. Assume reasonable values for thermal conductivities, T dependent
3. Utilize axial T_{cool}, with $T_{cool}^{in} = 500\,\text{K}$, reasonable flow rate, heat capacity, etc.
4. Utilize axial LHR, with $\text{LHR}_0 = 350\,\text{W/cm}$
5. Solve temperature profile for cladding surface, fuel surface, fuel centerline
6. Find axial location of peak centerline temperature

1.4. Part III Deliverables

1. Include effects of thermal expansion, densification, and fission product-induced swelling.
2. Simulate until gap closure, but do not need to handle contact.
3. Assume uniform, constant LHR.
4. Assume T and burnup-dependent thermal conductivity k_{th}.
5. Make appropriate assumptions where needed.
6. Determine the displacements and stress state in the fuel as a function of time.
7. Perform appropriate analyses: thermal stresses, cracks in fuel, gap closure, etc.

2. Methodology

Per the specifications of the assignment, for all of the simulations, the system geometry was configured in a two-dimensional, RZ-plane. The system was assumed to be axisymmetric with constant density throughout the materials and constant specific heats.

2.1. Mesh Refinement Studies

Two different geometries have been constructed for analysis in this project, with their meshes determined utilizing the following procedure. Various options of mesh coarseness were investigated during the preliminary stages of this project. An analytical solution was attained, and the mesh was refined and optimized until it showed a reasonable agreement with the calculated solution.

For the fuel pellet, it was found that the 600x8 mesh best suited the purposes. The y-intercept of the analytical solution is 1908.0182 K and the y-intercept of the refined 600x8 mesh is 1903.3958 K. This amount of agreement is sufficient to ensure that the MOOSE code faithfully calculates the physical processes ongoing in the system and is unaffected by issues that could come up due to under-refinement. (Figure 1)

For the fuel rod, an approximately peak centerline temperature value was known from the steady state temperature dependent thermal conductivity of the fuel pellet. The first option explored was a mesh of the same dimensions as applied for the fuel pellet, 600x8. A mesh study was performed by determining the radial temperature profile at the 50 cm height of the fuel rod (which notably is not the axial position of the peak temperature, but is quite close and was sufficient for this analysis. The centerline temperature of the fuel pellet was 1758.4290 K and the centerline temperature of the selected mesh was 1754.5774 K which was determined to be an acceptable agreement. The 625x50 mesh was chosen over the 650x50 mesh which showed nearly the same temperature profile because it utilizes less computational power to have a slightly less complex mesh. (Figure 2)

For the fuel pellet simulation which was utilized to model solid mechanical behavior and properties, a different method was taken towards modeling the gap. A mesh study was performed by analyzing the temperature profiles as calculated from a steady state simulation. (Figure 3) Notably, the agreement with the analytical solution is unfortunately limited as the meshes that were utilized involved temperature dependent thermal conductivities whereas the analytical methods were only suitable to accommodate constant thermal conductivity

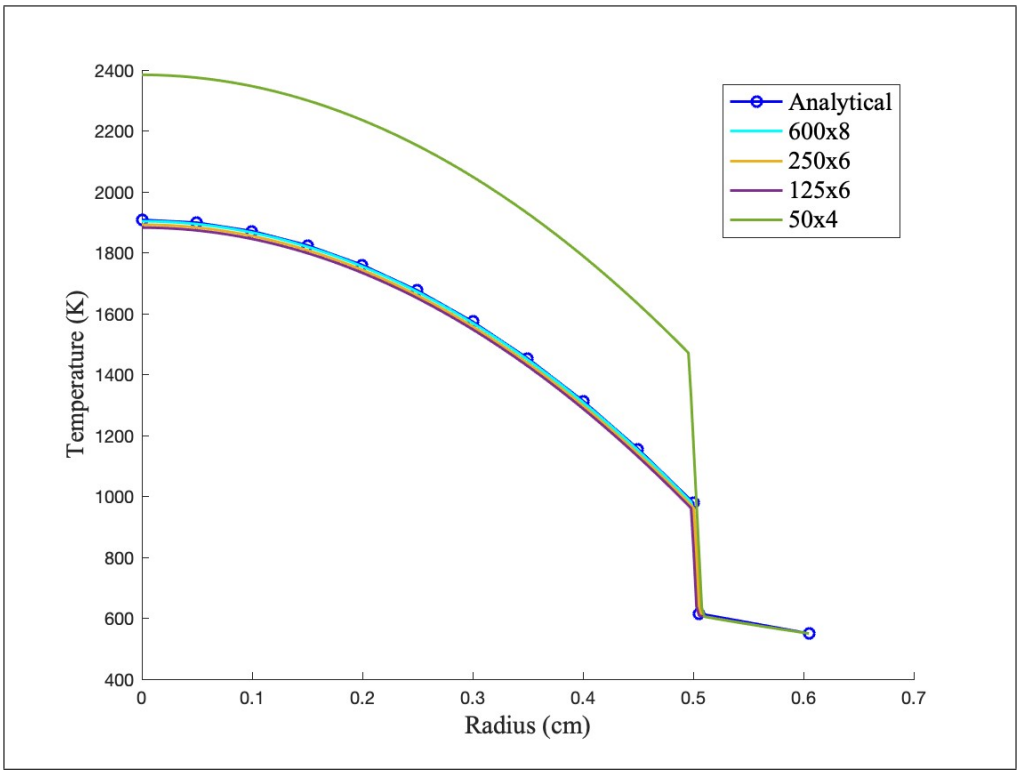

Figure 1: Four different options for mesh resolution compared with the analytical solution.

values for the fuel and the cladding. However, the mesh resolution which was ultimately selected utilizing nx = 100 and ny = 50 was chosen for its more seamless fit and general agreeance with the trend. It was verified that the tolerances were not a contributing factor to this difference, thus the centerline temperature difference may be attributed with certainty to the non-constant thermal conductivities utilized in these simulations. Additionally, due to the differently designated thermal conductivity of the gap and the burn up dependence of the thermal conductivity of the fuel as has been further discussed within the Materials Selection section of this report, the centerline temperature obtained here may not be compared to the other simulations for further verification. Effects of burn up at this stage in the simulation are quite minimal with the time of measurement was selected as 100 seconds to mitigate this source of error to the best extent possible.

2.2. Materials Selection and Properties

The materials were selected according to general industry standards. The selected fuel material, UO2, is the most common and most widely implemented fuel type. This fuel was assumed to be fresh with no thermal transport effects from burnup. The cladding was chosen as pure Zirconium due to the necessity of defining a temperature dependent relationship for the thermal conductivity coefficient and the accessibility of this parameter for this material. Generally, commercial reactors utilize Zircaloy-2 or Zircaloy-4 as their cladding materials. These options are both Zirconium-based alloys and have similar enough

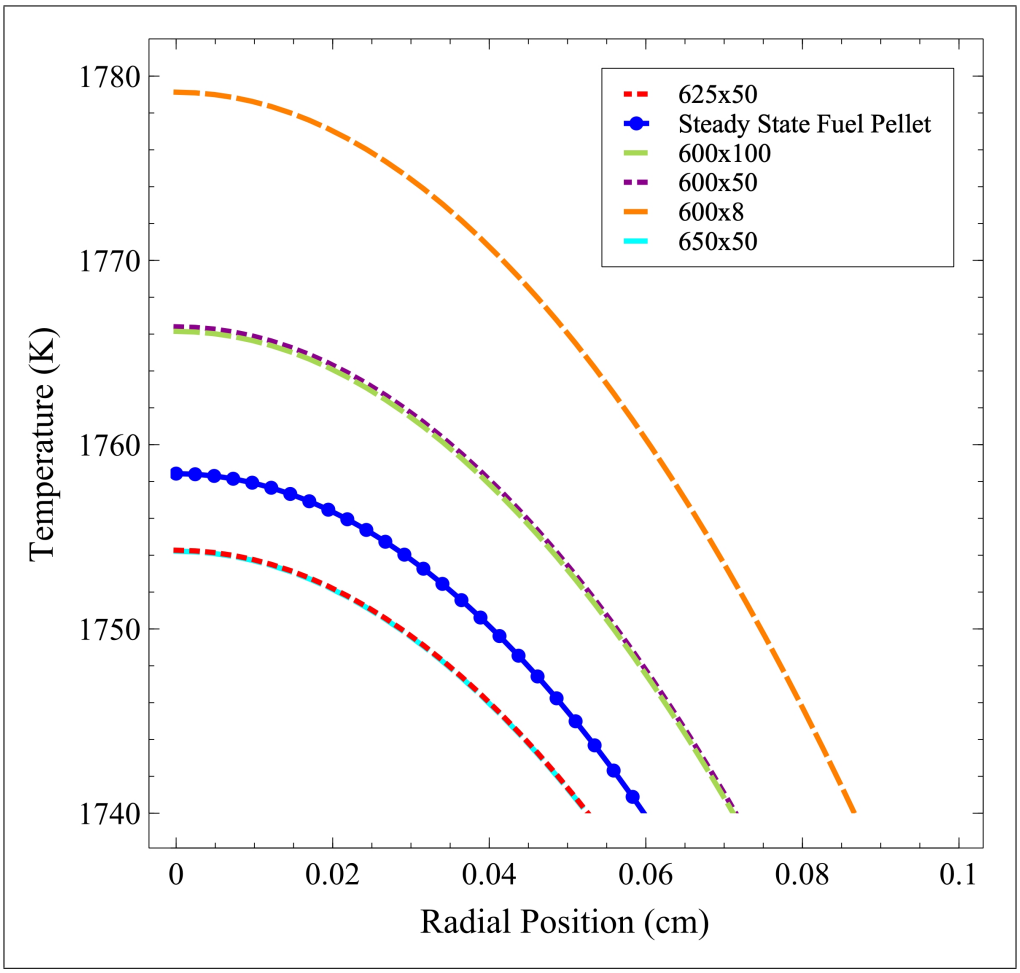

Figure 2: Five different options for mesh resolution as evaluated at Z_o compared with the steady state variable thermal conductivity fuel pellet solution.

heat transfer properties to pure Zirconium for this material to be a reasonable selection for a fuel cladding from a thermal transport perspective. Finally, the gap contained a pure Helium backfill, which, being an inert and lighter gaseous species, has desirable properties for nuclear reactor applications and is the typical option in commercial reactors. Because the fuel is assumed to be fresh, no considerations must be taken for fission gas release such as Xenon that would degrade the thermal transport efficiency. The material properties utilized for the systems with constant thermal conductivities or constant solid mechanical properties were found in the provided course material (Table 1) (Table 2). The temperature dependent thermal conductivity coefficients were found through studies as well as in the course material. [2] [3]

2.3. Fuel Pellet

Both a steady state and a transient condition were analyzed for the fuel pellet. A Dirichlet boundary condition was defined for the constant outer cladding temperature of

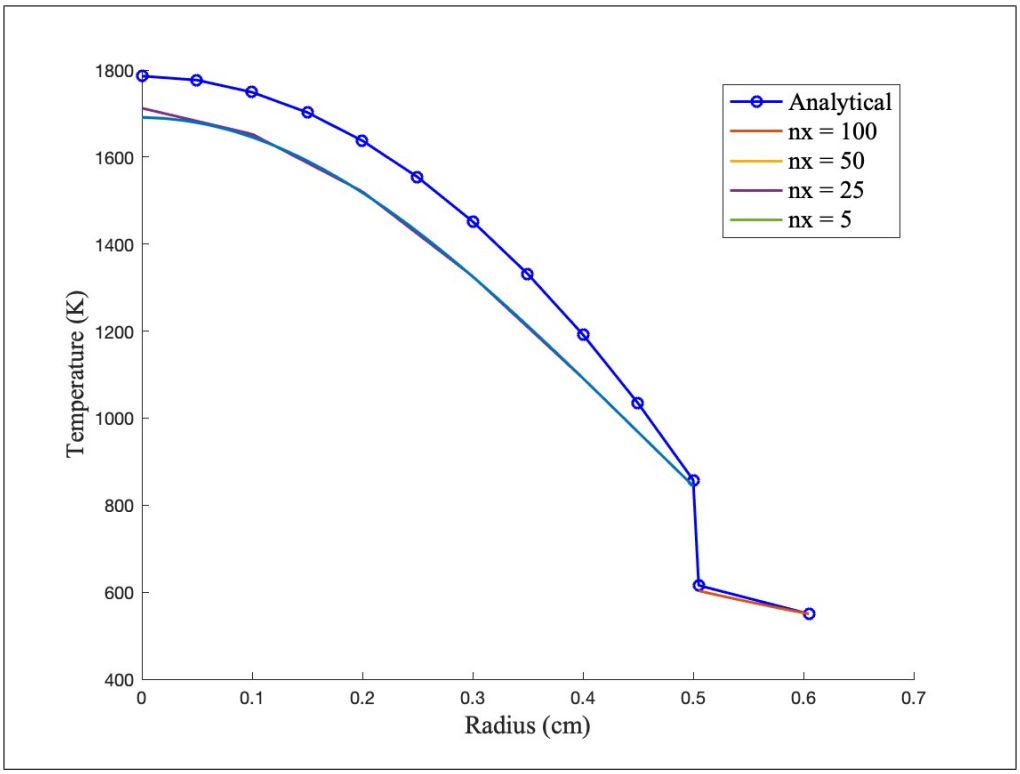

Figure 3: Solid mechanics fuel pellet mesh study.

Material	$\mathbf{k}_{th}$ **(W/cm-K)**	$\mathbf{c}_p$ **(J/g-K)**	ρ **(g/cm^3)**
Fuel: UO_2	0.03	0.33	10.97
Gap: He	1.53E-3	5.1932	1.786E-4
Clad: Zr	0.17	0.35	6.5

Table 1: Constant material property values.

Material	**E (GPa)**	ν	α **(10^{-6} K^{-1})**
Fuel: UO_2	200	0.345	11
Clad: Zr	80	0.41	7.1

Table 2: Constant solid mechanical material property values.

550 K. The steady state simulation was run with a constant VHR (1) defined as a heat source in the fuel subdomain of the mesh.

$$\text{VHR} = \frac{350}{\pi \cdot (0.5)^2}\,\text{W/cm}^3 \tag{1}$$

For the transient simulation, a function of LHR was provided and then converted into a volumetric heating rate (2) (Figure 3).

Material	$\mathbf{k_{th}(T)\ (W/cm\text{-}K)}$
Fuel: UO_2	$\left(\frac{100}{7.5408+17.629\left(\frac{T}{1000}\right)+3.6142\left(\frac{T}{1000}\right)^2}+\frac{6400}{\left(\frac{T}{1000}\right)^{\frac{5}{2}}}\exp\left(\frac{-16.35}{\frac{T}{1000}}\right)\right)/100$
Gap: He	$16\times10^{-6}\cdot T^{0.79}$
Clad: Zr	$\left(8.8527+7.0820\times10^{-3}\cdot T+2.5329\times10^{-6}\cdot T^2+2.9918\times10^{3}\cdot\left(\frac{1}{T}\right)\right)/100$

Table 3: Temperature dependent thermal conductivity coefficients

$$\mathrm{VHR}=\frac{350\cdot\exp\left(-\frac{(t-20)^2}{2}\right)+350}{\pi\cdot(0.5)^2}\ \mathrm{W/cm^3} \tag{2}$$

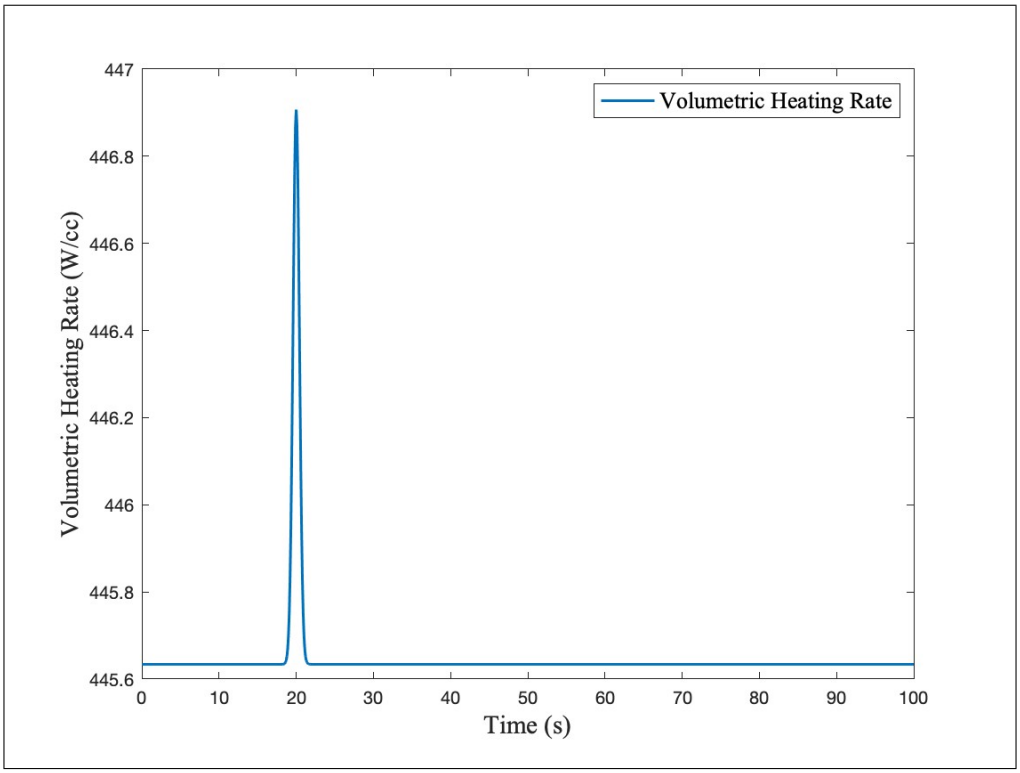

Figure 4: Volumetric Heating Rate function as derived from (2).

2.4. Fuel Rod

A steady state simulation was utilized to gain information on temperature profiles of a 100 cm long fuel rod with the same radial properties as the fuel pellet. The axial LHR (3)

was converted to a volumetric heat rate and implemented as a heat source throughout the fuel portion of the mesh. (Figure 4) The Z_o value is defined as half the total length of the fuel rod, making it 50 cm. The LHR^o value of 350 W/cm was assumed as outlined within the Part II Deliverables. This function notably peaks at the Z_o value.

$$LHR\left(\frac{z}{Z_o}\right) = LHR^o \cos\left[\frac{\pi}{2\gamma}\left(\frac{z}{Z_o} - 1\right)\right] \tag{3}$$

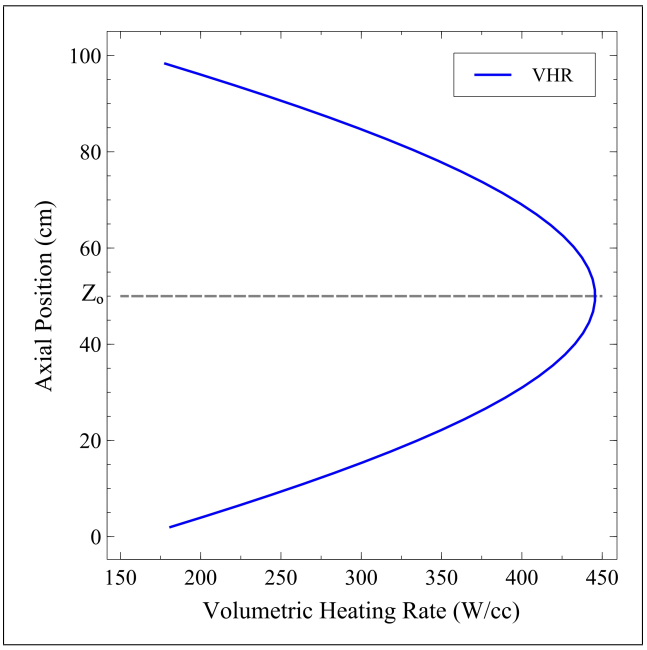

Figure 5: Volumetric heating rate function as derived from (3).

For the coolant interaction characterization, reasonable values were assumed for the coolant material properties including a specific heat capacity (c_p) of 4.2 J/g-K and a mass flow rate ($\dot{m}$) of 250 kg/s, a h_{cool} of 2.65 W/cm^2-K, and the parameter of $\pi/(2\gamma)$ was approximated as 1.2. [5] The temperature differential axially was determined through utilizing the T_{cool}^{in} of 500 K and applying the previously described parameters to (3) and applying the axial LHR (4) to solve for the temperature of the outer surface of the fuel cladding (5).

$$T_{cool} - T_{cool}^{in} = \frac{1}{1.2}\frac{Z_o \times LHR^o}{\dot{m}C_{PW}}\left\{\sin(1.2) + \sin\left[1.2\left(\frac{z}{Z_o} - 1\right)\right]\right\} \tag{4}$$

$$T_{co} - T_{cool} = \frac{LHR}{2\pi R_{fuel} h_{cool}} \tag{5}$$

The derived function was then defined as a Dirichlet boundary condition on the outer surface of the fuel cladding to approximate the effect of coolant entering from the 0 cm position, which would physically relate to the coolant's entrance into the core, to the 100 cm position, which would relate to its exit out of the core.

$$500+\frac{1}{250}\times\frac{1}{4.2}\times350\times50\div1.2\times\left(\sin(1.2)+\sin\left(1.2\left(\frac{z}{50}-1\right)\right)\right)+\frac{350\cos\left(1.2\left(\frac{z}{50}-1\right)\right)}{2\pi\times0.5\times2.65} \quad (6)$$

2.5. Solid Mechanics Considerations

In order to appropriately analyze the stress states present within the fuel as a result of thermal expansion and burn up, it was necessary to account for the different factors contributing to the volume change within the fuel pellet. (7) Within the program, there are terms accounting for general temperature-dependent thermal expansion, densification of the fuel pellet, solid fission product swelling, and gaseous fission product swelling. The following formulas for each respective item were provided within the course material. [5]

$$\epsilon_{\text{tot}} = \epsilon_{\text{th}} + \epsilon_{\text{D}} + \epsilon_{\text{sfp}} + \epsilon_{\text{gfp}} \quad (7)$$

The following is an analytical computation of the hoop, axial, and radial stress states. It may be observed that hoop stress is expected to be a larger tensile stress than the other two stress states.

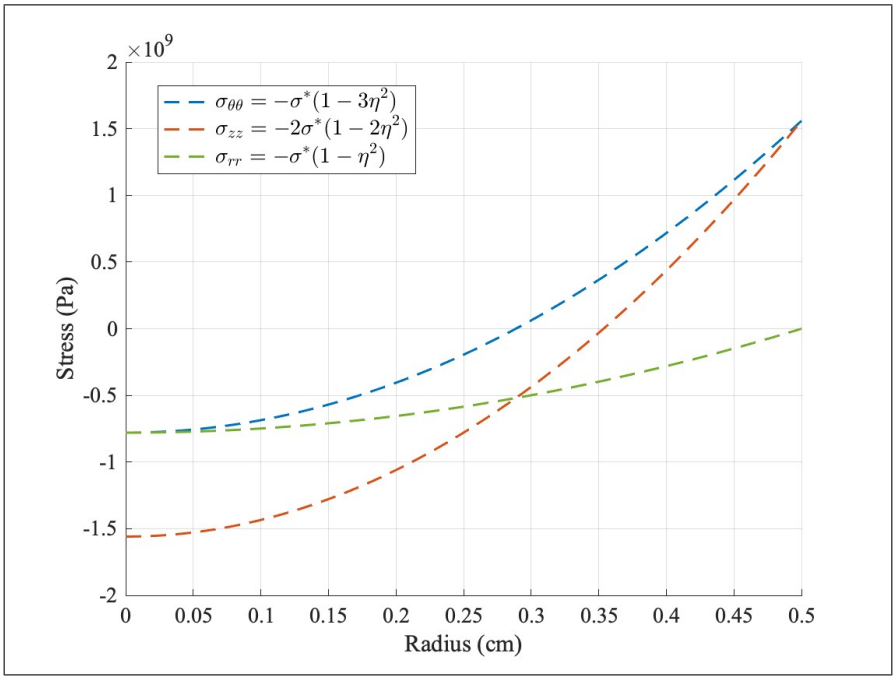

Figure 6: Analytically calculated hoop, axial, and radial stress states under normal LHR induced temperature gradient prior to volumetric changes.

2.6. Computational Methods

The following section details a summary of the input scripts and the settings therein that were written for this assignment. The variable of temperature was utilized because this is the property being analyzed in this study. Spatial variables and the variable of time do not need to be defined in MOOSE. The Kernels of Heat Conduction, Heat Source, and - for the transient systems – the Heat Conduction Time Derivative was utilized. For the transient simulations, the specific heat and density and heat conduction time derivative was needed as this is the left side of the governing equation used by MOOSE to analyze this problem. [1] Parsed Functions were utilized both to define the VHR and for the variable thermal conductivity coefficients. The Dirichlet boundary conditions were defined according to the specifications of the assignment. A Neumann boundary condition was defined for the assumption of no heat flux through the centerline of the fuel. Generic Constant Material was used for the simulations that did not require a variable definition for the thermal conductivity coefficient. Heat Conduction Material in conjunction with Parsed Function was utilized to define the temperature dependent expression for thermal conductivity coefficient. The preconditioning utilized the solve type of NEWTON because in the preliminary testing of the simulations, it was found that the PJFNK solve type had some difficulty converging. Postprocessor parameters were appropriately defined to gather the requested information for each simulation type. The steady state simulations utilized the Line Value Sampler to gather the temperature properties in the radial and axial directions in order to plot the temperature profiles. The transient simulations utilized Point Value because the property of interest was the fuel pellet centerline temperature as it changed over time, and the point was defined appropriately for this analysis. In the Executioner section, the absolute tolerance was adjusted for the transient simulations in order to enable efficient completion of the simulation runs without encountering errors. This adjustment was found to be permissible by analyzing the output files and confirming that they provided expected values and correlated with their respective steady state simulation results (respectively denoting the type of thermal conductivity constant utilized in each).

For the solid mechanical applications, several new actions and blocks were incorporated within the code. This is a summary of the selected items and methods utilized for this application. A new mesh structure was created for this problem, in order to more appropriately model the physical system of the fuel and cladding, the mesh which previously was in the place of the gap was removed. The fuel had a mesh and the clad had a mesh, each of which were positioned in space such as to have a 0.0500 cm gap between them at the start of the simulation. Different areas of the mesh were "labeled" for use later. Global Parameters of the displacements of the spatial variables were defined to prepare their application in the Boundary Conditions. The Physics, SolidMechanics, QuasiStatic actions were nested within one another to specify the desired outputs, namely for this assignment: the stress state of the fuel. Eigenstrains were defined for use later in the Materials block. In the Functions block, the burn up function is defined [5] and then passed into the thermal conductivity of the fuel. This function is dependent both on burn up and temperature. They are separately defined due to the nature of the way ParsedFunction has been designed throughout this project, designating "t" as temperature, but because MOOSE also recognizes "t" as time

and it cannot simultaneously be both, the burn up function is defined using it as time and then passed into the thermal conductivity function which uses it as temperature. Boundary Conditions (BCs) are defined, preventing the fuel clad from moving away in the x-direction and also imposing a reflecting boundary condition on displacements in the y-direction. This meant that the geometry above this BC would be reflected, thus the height of the fuel pellet within the mesh was halved for this particular simulation. Material properties were applied appropriately utilizing the previously described properties (Table 1) (Table 2). The implementation of gap conductivity may be found within the Constraints action and the UserObjects action. The gap conductance is approximated as 0.0023 because this value was verified to yield reasonable behavior and avoided making a fully temperature dependent gap conductance (which was quite computationally arduous). This approximation came from applying T = 550 K to the variable thermal conductivity equation for He gas (Table 3).

3. Results and Discussion

3.1. Fuel Pellet: Constant Thermal Conductivity Coefficient

The steady state simulation with constant thermal conductivity material properties utilized a constant (1) as a model for the heat source. The snapshot temperature profile (Figure 4) was taken at 100 seconds. The various regions of the temperature profile may be easily identified as the first region (0, 0.5) representing the oxide fuel, the second region (0.5, 0.505) shows the Helium gap with the poorest thermal conductivity properties as signified by the large temperature difference at the surface of the fuel and the inner cladding, and the third and final region (0.505, 0.605) shows the cladding. As previously stated, the centerline temperature for the steady state simulation with a constant thermal conductivity coefficient is 1903.3958 K.

For the analytical solution, the temperature of the fuel with respect to the radial position in the fuel pellet is modeled by an equation from the course material (2).

$$T_f = \frac{\text{LHR}}{\pi \cdot R_f^2} \cdot \frac{(R_f^2 - r_f^2)}{4 \cdot k_{\text{fuel}}} + T_s \,\text{K} \tag{7}$$

The transient simulations were run with a time-dependent VHR (2) from within the fuel block in the mesh. The maximum time-step was 0.5 and the tolerances in the Execution block were increased compared to what they were for the steady state runs to permit completion of the 100 second transient run.

The VHR peaks at 20 seconds at a value of 446.9071 W/cc. (Figure 3) The transient simulation centerline temperature had a peak of 2087.6336 K at 22.5 seconds, which is the appropriate response to the VHR reaching a higher value at 20 seconds. At 20 seconds, the centerline temperature instantly begins to increase. After this condition, the temperature reduces and equilibrates to 1903.4146 K. (Figure 6)

3.2. Fuel Pellet: Temperature Dependent Thermal Conductivity Coefficient

The temperature dependent thermal conductivity coefficients (Table 3) were utilized in two of the simulations to investigate the enhancement of thermal conductivity as temper-

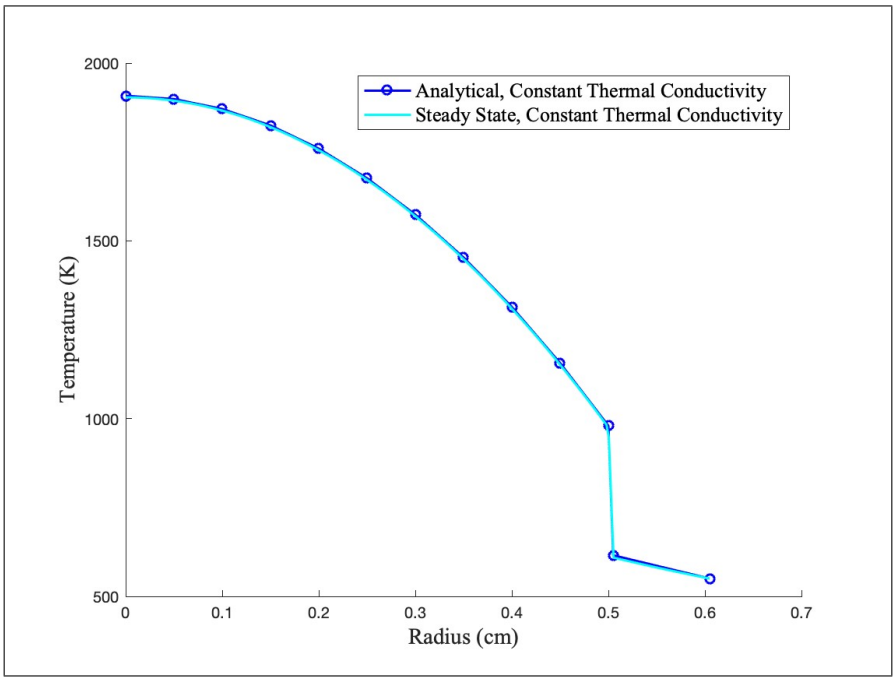

Figure 7: Analytical vs Steady State radial temperature profiles using constant thermal conductivity.

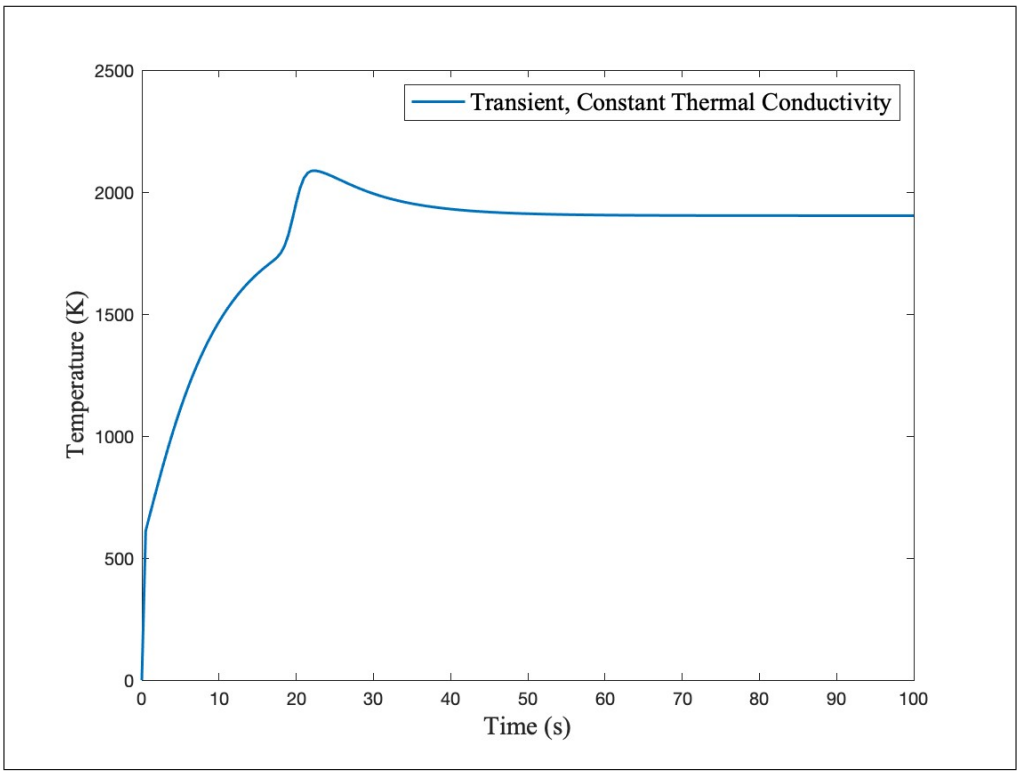

Figure 8: Fuel centerline temperature with constant k_{th}

ature increases. This effect is important because it ultimately lowers the fuel centerline temperature, which is a very important parameter in safety analyses and is instrumental to understanding the conditions in the fuel rods of a reactor.

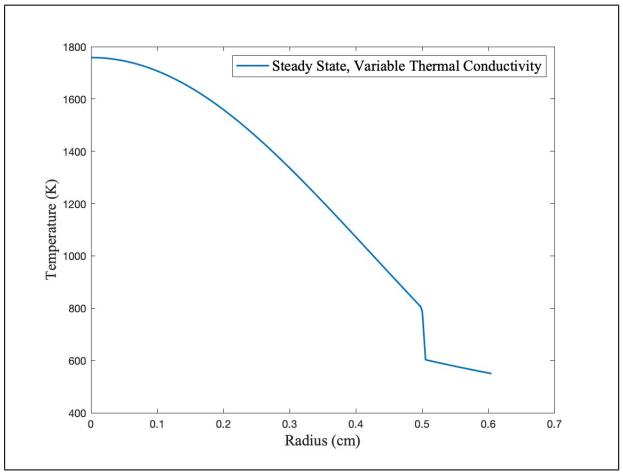

Figure 9: Fuel temperature profile with variable k_{th}.

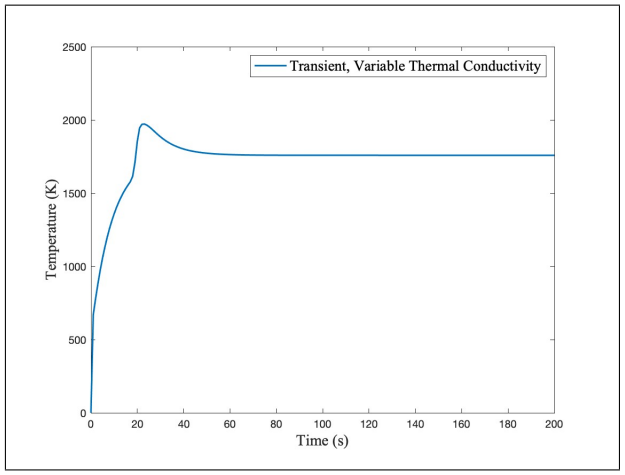

Figure 10: Fuel centerline temperature with variable k_{th}.

UO2's thermal conductivity coefficient decreases as temperature increases due to the effects of phonon scattering. However, the other two materials become more efficient at conducting heat which dramatically decreases the fuel surface temperature and decreases the fuel centerline temperature. In the steady state simulation, the peak temperature can be found to be 1758.4290 K. (Figure 7) In the transient simulation, the peak can be observed at 23 seconds with a value of 1971.6766 K. It equilibrates to a value of 1758.4290 K. (Figure 8) This shows excellent agreement with the steady state variable thermal conductivity value.

3.3. Fuel Rod: Axial Temperatures

The inner and outer fuel cladding surface temperature profiles of the fuel rod (Figure 9) show the implemented boundary condition (6) which is the same as the outer surface temperature and result of the heat transfer through the cladding from the heat source and sink. The maximum for the outer cladding coolant boundary condition occurs at a value of 557.2130 K at 63.8191 cm. This accounts for the lower coolant temperature in and the fact that it will emerge from the core at a higher temperature. For a typical power reactor, a much larger temperature difference is observed, but it must be noted that this is only one isolated fuel rod and unlike a typical power reactor with assemblies that are around 4 meters tall, this fuel rod is only 1 meter tall. These are possible explanations for the exiting coolant only increasing by a relatively small margin according to this model.

It is notable that the axial positions at which the peak temperatures occur are slightly shifted above the Z_o position (closer to the outlet of the core) where the peak originally occurred in the implemented VHR function (Figure 4). The reason the peaks are shifted is because the thermal conductivity is much higher near the center of the fuel rod due to the larger difference in temperature between the inlet coolant and the hottest region of the rod

but as the temperature of the coolant increases, this heat transfer becomes less efficient due to the fundamental laws of thermodynamics. Less thermal conductivity makes the inner clad surface a higher temperature as we are still in a high temperature region of the core but the driving mechanism of the temperature differential has been reduced.

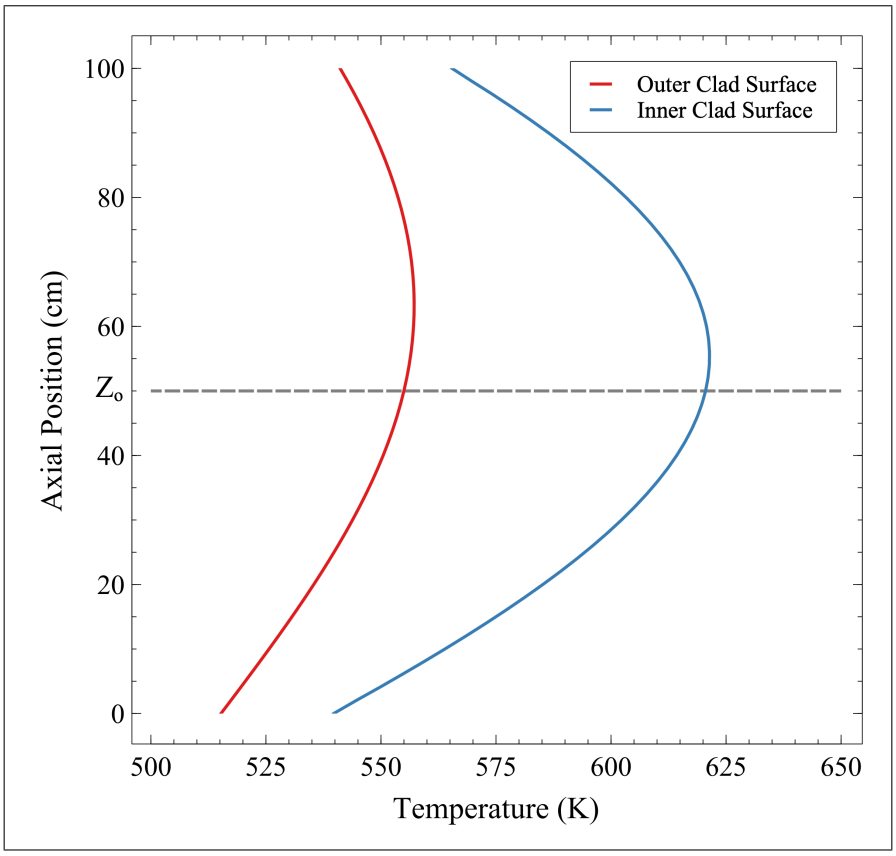

Figure 11: Inner cladding surface and outer cladding surface axial temperature profiles.

The temperature profiles of the inner cladding surface, fuel surface, and fuel centerline are all as expected. (Figure 10) The axial position of the peak fuel centerline temperature occurs at 50.7538 cm at the previously mentioned value of 1754.3399 K. The peaks progressively shift closer to the Z_o value as they are closer to the fuel because this is much closer to where the VHR function is being applied and thus, the bias inflicted by the outer cladding temperature's skewed peak is less significant as we move away from where the heat sink is and towards the heat source.

As representative of their material properties, the heat transfer between the fuel surface and the inner cladding is relatively poor due to the gap while the heat transfer between the fuel centerline and the fuel surface is comparatively much better. Additionally, the temperature of the centerline on the edges of the fuel rod (as predetermined by the VHR) represent the lower thermal neutron flux found in those regions due to their location on the periphery where they are only surrounded by fissile material on their innermost side. This is intuitive, as one would not - under desired circumstances - expect neutron flux to be

produced within the coolant.

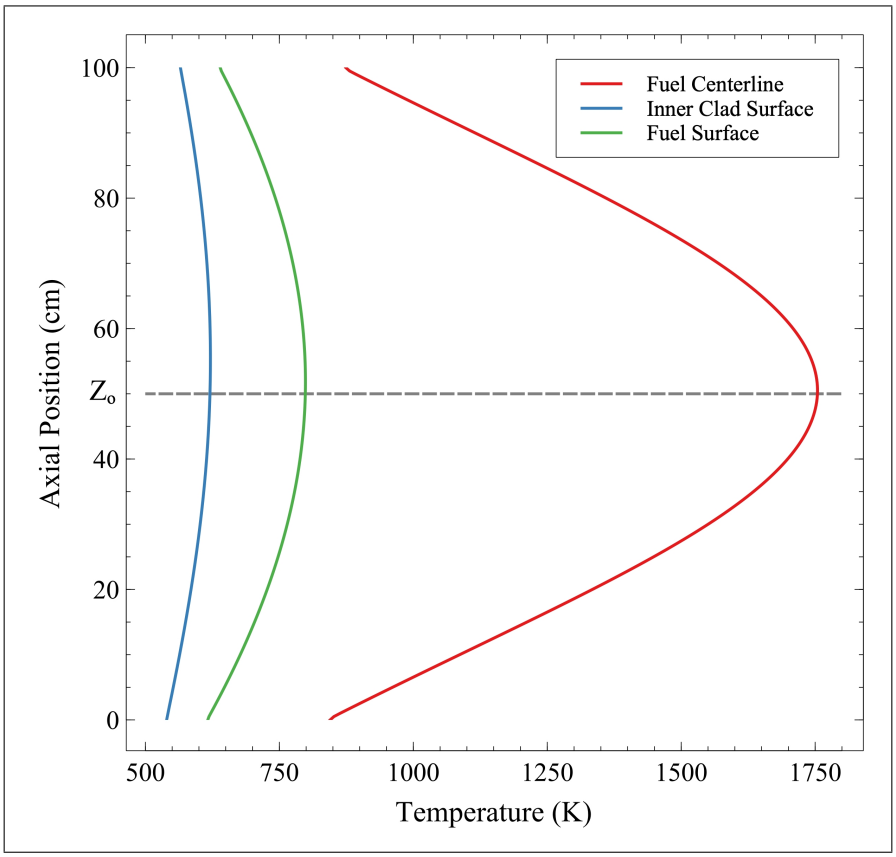

Figure 12: Inner cladding surface, fuel centerline, and fuel surface axial temperature profiles.

3.4. Fuel Pellet: Solid Mechanics

It was found utilizing methods of simple linear interpolation that at time t = 59,896,175.246 seconds (693.32 days) gap closure (gap width equal to 0 cm) is achieved. One may observe that the effects of densification substantially delayed the full closure of the gap. (Figure 12) Additionally, the simulation generally represents the physical behavior faithfully by not allowing the pellet and the cladding to substantially overlap following their contact, a property which the horizontal plateau at 0 cm is indicative of.

The temperatures of the fuel centerline and fuel surface in relation to time may be collected. (Figure 13) It may be observed that as the gap first widens slightly due to the densification of the fuel, the temperatures experience an increase. This is because of the low thermal conductivity of the gap in comparison to the fuel and cladding, so having a greater distance to travel in the x-direction to transfer the heat will result in more heat staying within the pellet. When the gap begins to shrink, the heat transfer becomes more efficient, as may be observed by the temperatures decreasing (indicative that more heat is now escaping to the coolant and the temperature distribution is becoming more uniform). Once the gap closes (as indicated by the black dashed line), the temperatures become constant because

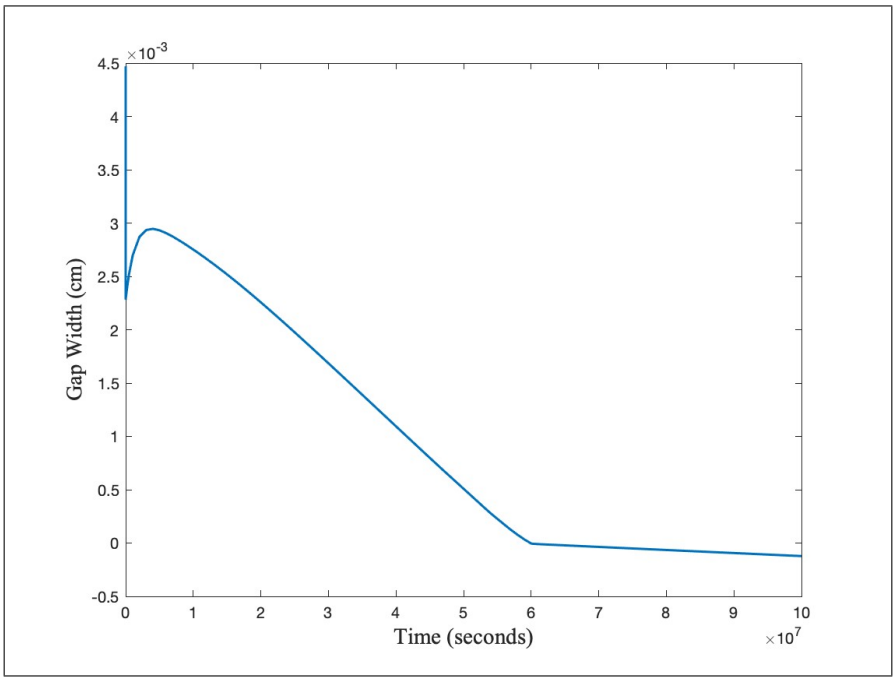

Figure 13: Fuel-Cladding gap width as a function of time.

there is a constant heat generation rate and there is no more change to be made in the efficiency of thermal conductivity of the system.

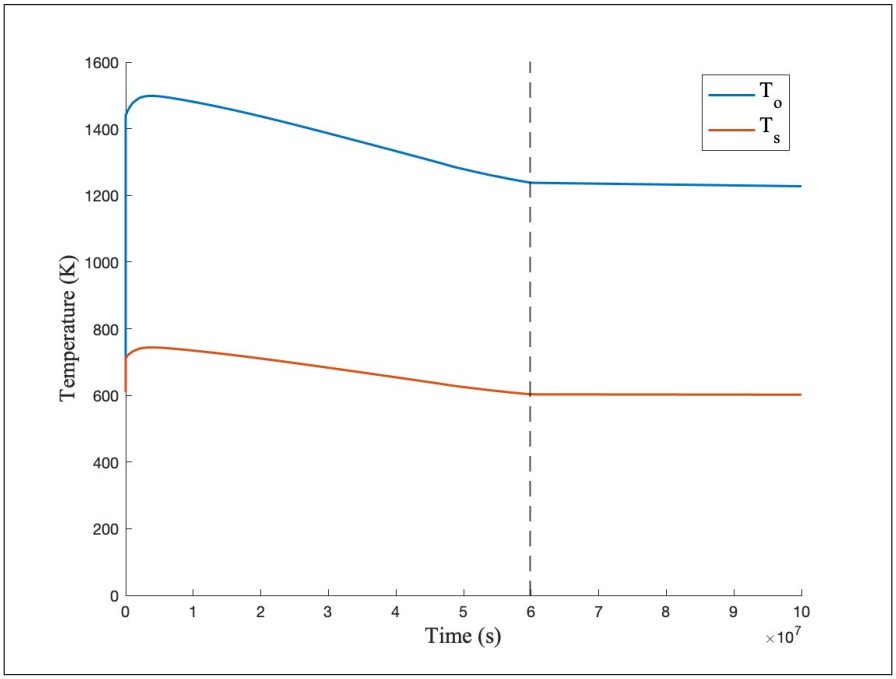

Figure 14: Temperatures of fuel pellet centerline (T_o) and fuel pellet surface (T_s) in relation to time (s).

So as to observe the stress state of the fuel in relation to time, the radial, axial, and hoop stresses have been collected. (Figure 14) The hoop stress within the system as it is defined in the simulation corresponds to the σ_{zz} values. Its maximum value occurs 909.78 MPa. This means the cracks extend into the fuel a distance of 0.3119 cm. This value was derived using the maximum hoop stress value, as well as constant material parameters (Table 1) (Table 2) and the appropriate formulas as seen below.

$$\Delta T = \frac{LHR}{4\pi k}$$

$$\sigma^* = \frac{\alpha E \Delta T}{4(1-v)}$$

$$\eta = \sqrt{\frac{1}{3}\left(1 + 909779816.281250\right)/\sigma^*}$$

$$r = R_f \eta = 0.3119\,\text{cm}$$

The hoop stress and radial stress become compressive after 986.76 days due to the gap closure and the effects of the cladding pushing back on the outer sides of the pellet such that the net values become negative.

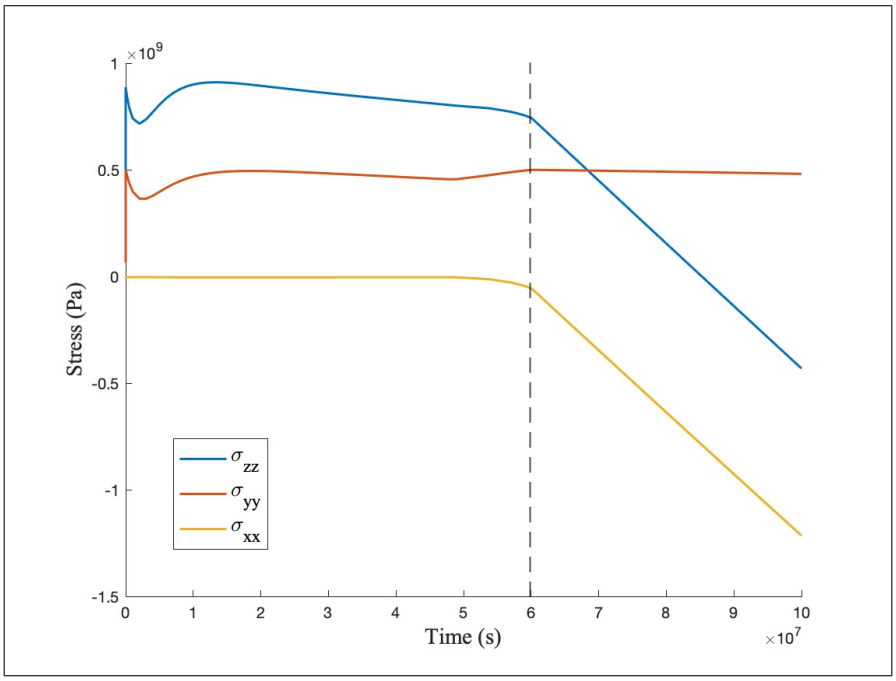

Figure 15: Fuel-Cladding gap width as a function of time.

Conclusion

In summary, the following thermal and mechanical analysis of fuel systems yielded meaningful results for thermal and solid mechanical behaviors of fuel pellet and fuel rod systems. MOOSE is evidently a reliable tool for predicting the behaviors of materials with well understood material properties under stresses and temperature gradients and continues to inform the engineering of fuel systems and the evaluation of fuel performance.

References

[1] Guillaume Giudicelli, Alexander Lindsay, Logan Harbour, Casey Icenhour, Mengnan Li, Joshua E. Hansel, Peter German, Patrick Behne, Oana Marin, Roy H. Stogner, Jason M. Miller, Daniel Schwen, Yaqi Wang, Lynn Munday, Sebastian Schunert, Benjamin W. Spencer, Dewen Yushu, Antonio Recuero, Zachary M. Prince, Max Nezdyur, Tianchen Hu, Yinbin Miao, Yeon Sang Jung, Christopher Matthews, April Novak, Brandon Langley, Timothy Truster, Nuno Nobre, Brian Alger, David Andr, Fande Kong, Robert Carlsen, Andrew E. Slaughter, John W. Peterson, Derek Gaston, Cody Permann, Enabling massively parallel Multiphysics simulations, SoftwareX, Volume 26, 2024, ISSN 2352-7110.
[2] J.K. Fink, L. Leibowitz, Thermal conductivity of zirconium, Journal of Nuclear Materials, Volume 226, Issues 1–2, 1995, ISSN 0022-3115.
[3] Kuzmin, Arian, Yurkov, M. (2017). Thermal conductivity coefficient UO_2 of theoretical density and regular stoichiometry. MATEC Web of Conferences, 92, 01050.
[4] Maheshwari, Saraswat, Vineet, Kumar, Jitendra, Alam, Zafar, Hafiz, Adnan. (2021). TEMPERATURE PROFILE AND THERMAL PERFORMANCE OF BOILING WATER REACTOR BASED POWER PLANT.
[5] General Course Material